

Magnetoelectric composites of nickel ferrite and lead zirconate titanate prepared by spark plasma sintering

Q.H. Jiang^a, Z.J. Shen^{b,*}, J.P. Zhou^a, Z. Shi^a, Ce-Wen Nan^{a,*}

^a State Key Laboratory of New Ceramics and Fine Processing, and Department of Materials Science and Engineering, Tsinghua University, Beijing 100084, China

^b Department of Inorganic Chemistry, Arrhenius Laboratory, Stockholm University, SE-106 91 Stockholm, Sweden

Received 11 January 2006; accepted 17 February 2006

Available online 18 April 2006

Abstract

Magnetoelectric (ME) bulk composites of ferrite and lead zirconate titanate (PZT) were prepared by spark plasma sintering (SPS) of mechanically mixed ferrites, BaFe₂O₄ or NiFe₂O₄ and a soft lead zirconate titanate, PZT-5A, powders. The feasibility of retarding possible reactions occurring between the ferrite and lead zirconate titanate was approved by applying such a dynamic process as SPS. It was further revealed that nickel ferrite and PZT-5A is a more favorable combination that underwent no obvious reactions up to 1050 °C. Efforts were made to optimize the SPS processing parameters in order to produce immiscible composites with high electrical resistivity, low dielectric loss and better magnetoelectric response.

© 2006 Elsevier Ltd. All rights reserved.

Keywords: Ferrites; PZT; Multiferroics; Composites; SPS; NiFe₂O₄; PZT

1. Introduction

The coexistence of ferroelectric and magnetic orders leads to magnetoelectric (ME) effect, which is defined as an induced dielectric polarization in a material under an applied magnetic field and/or an induced magnetization under an external electric field.¹ According to Hund's rule, the coupling of ferromagnetism collides with the strong covalent bonds necessary for ferroelectricity. This fact limits the possibility of the coexistence of ferromagnetism and ferroelectricity in single compounds, among which BiFeO₃,² AMnO₃³ and AMn₂O₅⁴ (with A representing rare earth elements) are the very few so far discovered compounds known as single phase multiferroics. These single-phase materials have attracted intensive academic interest, but are still far beyond the practices because they demonstrated very weak ME effect or/and low phase transition temperature. Another alternative approach to obtain multiferroics is to produce composites consisting of ferrite and piezoelectric phases.⁵ It has been reported that such composites

may exhibit a larger ME effect than the single-phase materials⁶ owing to the magnetic-mechanical-electric interaction between the piezoelectric and ferrite phases.⁷ The ME voltage coefficient is defined as $\alpha_E = E/H$ where E is the electric field produced by an applied magnetic field H . Many researchers have investigated the ME coupling behaviour in the piezoelectric/ferrite composites both experimentally and theoretically.^{8–10}

So far, the obtained piezoelectric/ferrite ceramic composites all demonstrated much smaller measured ME coefficients than what predicated by the theoretical calculations. The challenge remains in achieving sufficient bulk density whilst avoiding possible reaction between the constitutional phases to occur. In order to get magnetoelectric response close to the predicted theoretical values in ceramic composites some other obstacles need to be overcome as well. For instance, large thermal expansion mismatch between the piezoelectric and ferrite phases harms the densification and leads to the formation of microcracks; the application of high sintering temperature in conventional sintering processes yields the formation of unwanted phases by chemical reaction; and the inter-phase diffusion of the constitutional atoms, though difficult to verify, lowers the local eutectic point around the boundary region thus to facilitates the formation of high concentration of defects and liquid phases. The last two aspects would lead to low resistivity of the composites and thus

* Corresponding authors. Tel.: +86 10 62773587; fax: +86 10 62773587.

E-mail addresses: shen@inorg.su.se (Z.J. Shen), cwnan@tsinghua.edu.cn (C.-W. Nan).

¹ Tel.: +46 8 16 23 88; fax: +46 8 15 21 87.

the large leakage current and loss of piezoelectrically generated charges.

Spark plasma sintering (SPS) is an efficient sintering method that allows rapid consolidation at comparatively low temperatures, although the underlying mechanisms for an enhanced mass-transport within a limited period of time still remain to be understood.¹¹ By the dynamic features this sintering method was considered to be feasible for the fabrication of magnetoelectric ceramic composites with high density and purity. The short time and low temperature required for densification during SPS process diminish the possibility for unwanted reaction to occur.

2. Experiment

Submicron-sized BaFe₂O₄ (BFO), NiFe₂O₄ (NFO) and a soft lead zirconate titanate (PZT-5A) powders were selected as precursors. Both BFO and PZT-5A are commercial powders and were used as received without any further treatment before mixing. The NFO powder was laboratory synthesized by a sol–gel method.¹² The mixtures of x NFO/(1 – x) PZT with the volume fractions x varying from 0.3 to 0.5 were mixed by ball milling and consolidated in vacuum in an SPS apparatus (Dr. Sinter 2050, Sumitomo Coal Mining Co. Ltd., Japan). The powders were loaded into a cylindrical carbon die with an inner diameter of 12 mm. Heating was accomplished by passing a pulsed dc current through the uniaxially pressurised die assembly. The final sintering temperature was set between 900 and 1050 °C, with a holding time of 0–3 min. The temperature was automatically raised to 600 °C over a period of 3 min, and from this point it was monitored and regulated by an optical pyrometer focussed on the surface of the die. The heating rate between 600 °C and the sintering temperature was 100 °C/min. A uniaxial pressure of 50–100 MPa was applied. All SPS consolidated samples were subsequently annealed at 800 °C for 5 h in air to ensure full oxidation.

Densities of consolidated specimens were measured using the Archimedes method. Phase constitutions were identified by the X-ray powder diffraction (XRD) method on a Rigaku D/max-rB X-ray diffractometer. A scanning electron microscopy (JSM-6310F) was employed to analyze the microstructure and element distributions of the samples.

The samples were electroded by using a silver paint and then polarized in an electric field of 20 kV/cm at 30–80 °C. The piezoelectric constant, d_{33} , was measured with a standard piezo d_{33} meter. The dielectric properties were measured with an HP4194A LCR. The magnetoelectric effect was measured in terms of the of the magnetoelectric coefficient as a function of dc magnetic field H_{dc} . The sample was put into the dc magnetic field up to 0.5 T superimposed an ac parallel magnetic field dH . A signal generator drives the Helmholtz coil to generate the ac magnetic field. At the output voltage of 20 V, the ac magnetic field generated was variable with the frequency because of the coil impedance, for instance, $dH = 12$ Oe at the frequency of 1 kHz and $dH = 3.1$ Oe at 10 kHz. The charge generated from the samples was collected by a charge amplifier (DSC3062, Beijing, China). When the polarization direction was parallel to the dc magnetic field, the longitudinal magnetoelectric sensitivity α_{E33}

($=dE_3/dH_3$) was obtained; the transverse magnetoelectric sensitivity α_{E31} ($=dE_3/dH_1$) was measured when the polarization direction was perpendicular to the magnetic field.

3. Results and discussion

In order to verify the compatibility of ferrite and PZT phases during densification, the bilayered ferrite/PZT pellets were sintered at 950 °C for 3 min by SPS under a uniaxial pressure of 50 MPa. Two ferrite phases, BaFe₂O₄ and NiFe₂O₄, were used. Fig. 1 shows the SEM micrographs of the interface regions of the AFe₂O₄/PZT (with A representing either Ni or Ba) bilayered samples. For the NFO/PZT sample, the interface between the two layers is distinct (Fig. 1a), and there is no obvious inter-phase diffusion and reaction zone as shown in Fig. 1b. For the BFO/PZT sample, a visible inter-phase diffusion zone of about 20 μ m in width was formed between the two layers. Checked with energy-dispersive X-ray analysis (EDX), the needle-like phase had similar element content to PZT phase. This needle-like phase in this inter-phase diffusion zone was induced by the tiny diffusion of Ba and Fe. However, the content of Ba and Fe was not exactly quantitated with EDX. By this experiment the BFO was excluded whereas NFO was select as ferromagnetic phase in later fabrication of the 0–3 type particulate composites in order to get high magnetoelectric response.

3.1. Effect of SPS conditions

The composite of 0.3NFO/0.7PZT was consolidated under various sintering conditions as shown in Table 1. The sample sintered at 900 °C achieves ~97% of theoretical density (TD) and a high electrical resistivity. The leakage current is about 0.146 mA under the polarization voltage of 2 kV/mm at 80 °C in this sample. The sample can be polled easily and achieves a piezoelectric constant d_{33} value 40 pC/N. With the increase in the sintering temperature up to 950 °C, the relative density of the composite is further increased to close to 99% of TD. The electrical resistivity of the sample declines however, which makes the poling of the samples difficult and the reduction of d_{33} value down to 10 pC/N.

Fig. 2 shows the variation of the dielectric constant and loss with frequency at room temperature of the 0.3NFO/0.7PZT composite prepared under different SPS conditions. The observation of a high value of dielectric constant at low frequency can be explained by the space charge polarization due to the inhomogeneous dielectric structure in the ceramic composites. As the data listed in Table 1 revealed, higher sintering temperature and prolonged sintering time in general lead to high bulk density, but lower electrical resistivity, higher dielectric constant and loss. Apparently, the presence of a small quantity of pores favors the reduction of the leakage current and the microstructure tailored by sintering is pivotal in determining the dielectric properties.

The XRD patterns of the 0.3NFO/0.7PZT particulate composites prepared under different SPS conditions are shown in Fig. 3. All the diffraction peaks can be indexed to NFO and PZT phases, implying that no impurity phase appears in the compos-

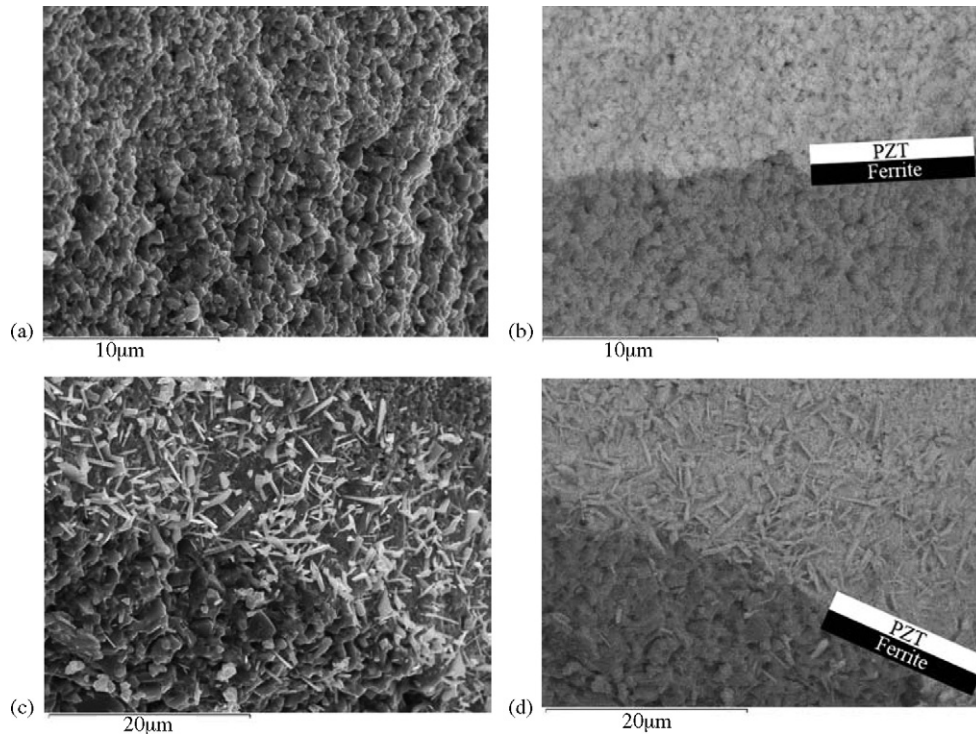


Fig. 1. The scanning electron microscopic (SEM) image revealing the interface between ferrite and PZT in laminated composites: (a) the secondary electron image; (b) the backscattered electron image of $\text{NiFe}_2\text{O}_4/\text{PZT}$; (c); and (d) the corresponding secondary electron image and backscattered electron image of $\text{BaFe}_2\text{O}_4/\text{PZT}$, respectively.

ites. Fig. 4 shows the SEM micrographs of the prepared samples. Fig. 4a is the backscatter modal SEM micrograph of sample No. 4 listed in Table 1. The EDX analysis confirmed that the regions with grey and dark contrast on polished surfaces represent the phase area of PZT and NFO, respectively. The monodisperse of particles was not achieved in the composites by mechanical mixing applied in the present study, instead NFO were observed to disperse in PZT matrix as aggregates. Fig. 4b is a secondary electron modal SEM micrograph of another sample with 50 vol.% of NFO. It reveals that the grain size in consolidated composites is submicron, implying the grain growth is restricted under the applied sintering conditions.

Fig. 5 shows that bias magnetic field H dependence of ME voltage coefficients (α_{E33}) for the 0.3NFO/0.7PZT bulk composites. α_E does not change monotonically with the magnetic field, but it increases with H to a peak value at H_m , followed by a rapid drop. The H dependence of α_E tracks the variation of

piezomagnetic coupling $q = d\lambda/dH$ (λ being magnetostriction). At the higher magnetic field, α_E is close to low value because λ goes near to be constant. It is known that the magnetoelectric coefficient can be calculated by the formula

$$\alpha = \frac{dE}{dH} = \frac{Q}{\varepsilon\varepsilon_0 S dH} = \frac{Q}{\varepsilon_0 S dH} \frac{1}{\varepsilon} \quad (1)$$

where Q is the charge generated from the samples which is collected by a charge amplifier; S is the area of the sample; dH is ac magnetic field; ε_0 is equal to 8.85×10^{-12} F/m. As the volume content of PZT in the samples is fixed to 70% and the change in d_{33} is ignored, Q is almost steady at a constant bias field. As a result, α is in proportion to $1/\varepsilon$ in the certain range. It is clear that the sample No. 4 has a stable low dielectric constant (Fig. 2) in the measured range, and thus it exhibits the largest magnetoelectric coefficient, as shown in Fig. 5.

Table 1

The relative density, poling condition, and d_{33} of the composites consolidated by SPS under different conditions

Label	Composition	SPS condition ^a	Density ^b (% TD)	Poling voltage (KV/mm)	Poling temperature (°C)	Leakage current (mA)	d_{33} (pC/N)
No. 1	0.3NiFe ₂ O ₄ /0.7PZT	1050/0/50	99.1	1.2	30	0.132	9.3
No. 2	0.3NiFe ₂ O ₄ /0.7PZT	950/3/50	99.1	0.5	30	0.170	10.6
No. 3	0.3NiFe ₂ O ₄ /0.7PZT	950/3/100	100	1	30	0.180	13.4
No. 4	0.3NiFe ₂ O ₄ /0.7PZT	900/3/50	97.0	2	80	0.146	40
No. 5	0.4NiFe ₂ O ₄ /0.6PZT	900/3/50	94.4	2	60	0.136	20
No. 6	0.5NiFe ₂ O ₄ /0.5PZT	900/3/50	89.2	2	60	0.204	15

^a Temperature (°C)/Holding time (min)/Pressure(MPa).

^b The theory density is 5.37 and 8.0 g/cm³ for NFO and PZT, respectively.

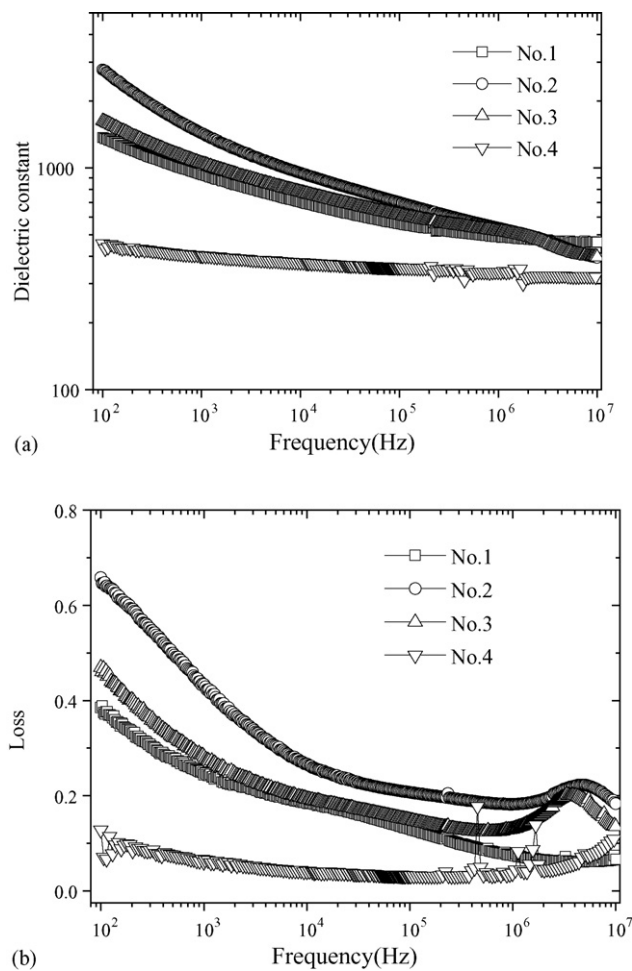


Fig. 2. The frequency dependence of the dielectric constant (a) and loss (b) of 0.3NFO/0.7PZT composite prepared under different sintering conditions.

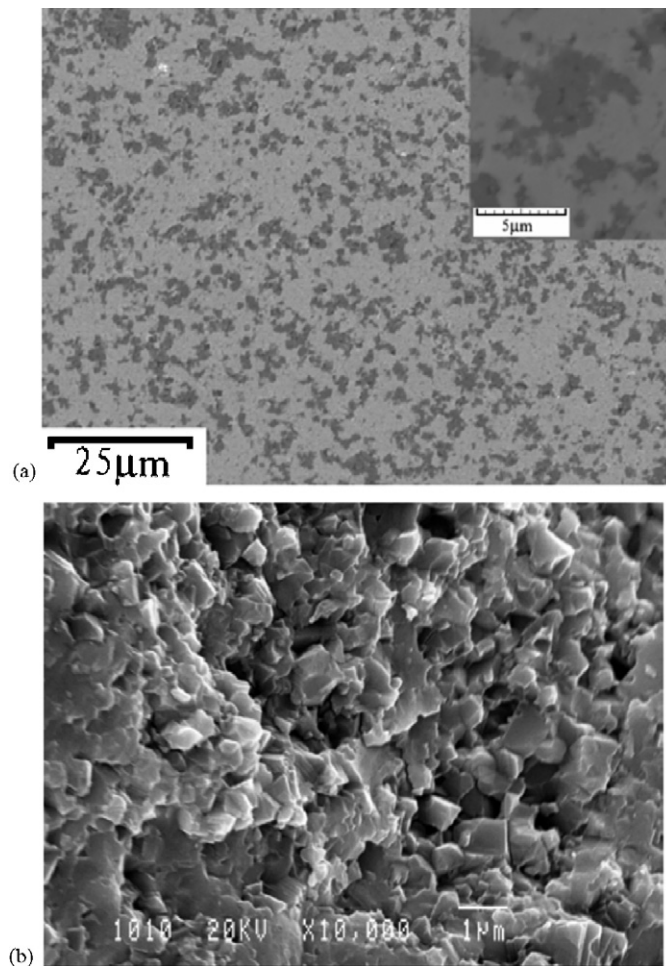


Fig. 4. The SEM images of the polished surfaces of the samples No. 4 (a) and of the fractured surface of the sample No. 6 (b) in secondary electron modal, revealing the phase distribution and the grain size and morphology in consolidated composites.

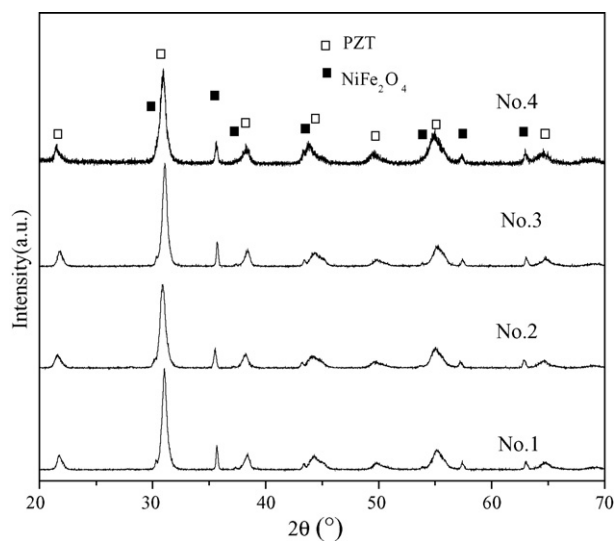


Fig. 3. The XRD patterns of the 0.3NiFe₂O₄/0.7PZT composite prepared under different sintering conditions.

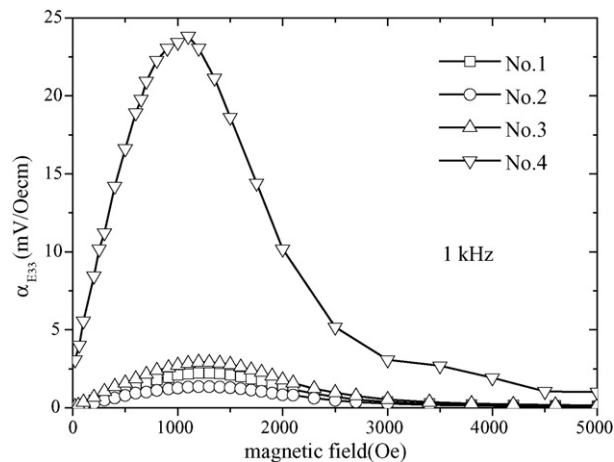


Fig. 5. Bias magnetic field H dependence of magneto-electric voltage coefficients (α_{E33}) for 0.3NFO/0.7PZT bulk composites at different sintering conditions.

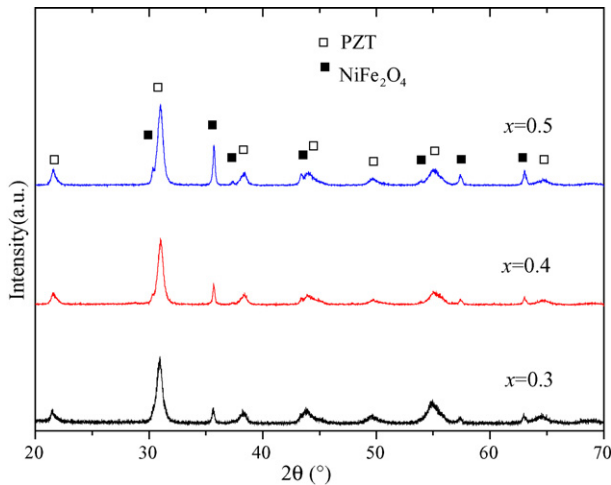


Fig. 6. The X-ray diffraction patterns of $x\text{NiFe}_2\text{O}_4/(1-x)\text{PZT}$ composites consolidated at 900°C for 3 min.

3.2. Effect of composition

The NFO/PZT mixtures with different NFO volume content were sintered under the same SPS condition, i.e., at 900°C for 3 min under 50 MPa. The XRD patterns of the compacted samples presented in Fig. 6 reveal that there coexist only NFO and PZT, and no impurity is observed. The dielectric constants of the composites were shown in Fig. 7. Because PZT is a high-permittivity dielectric material but the ferrite is a kind of semiconductor, the dielectric constant of the composites decreases, as expected, with the increase in the volume fraction x of NFO, see the inset of Fig. 7. The observed three electromechanical resonance peaks at 200, 400 and 2 MHz are originated from PZT, which become weaker with increasing x .

The piezoelectric constant of PZT and the magnetostriction of NFO are the two essential parameters that determine the magnetoelectric effect. The poling conditions and the piezoelectric constant d_{33} for these composites are shown in Table 1. With the increase of NFO phase content, the samples become more difficult to be polarized because the reduction of their elec-

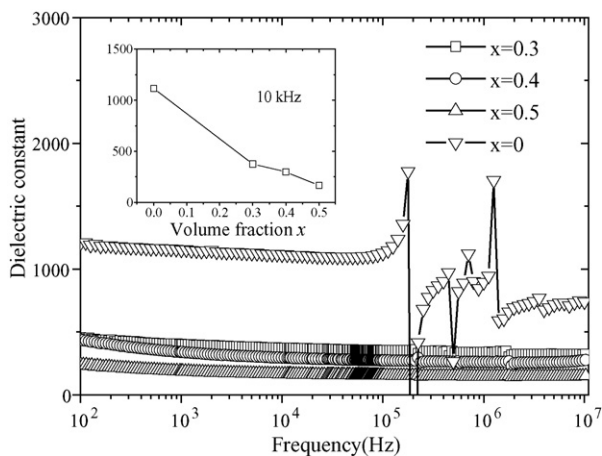


Fig. 7. The frequency dependence of the dielectric constant measured for $x\text{NFO}/(1-x)\text{PZT}$ composites. The inset shows the dielectric constant of the composites as a function of the volume fraction x of NFO.

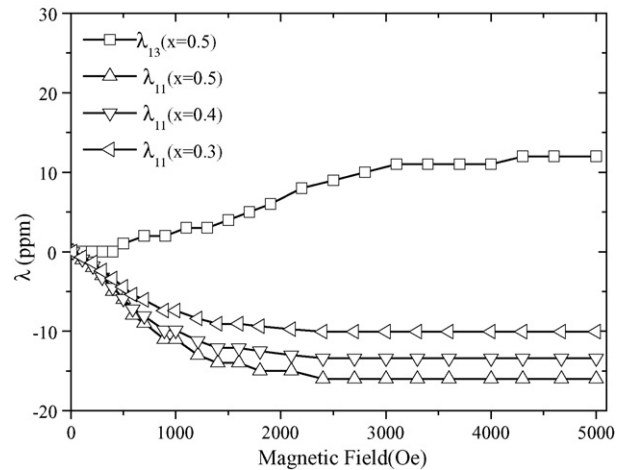


Fig. 8. Magnetostriction on $x\text{NFO}/(1-x)\text{PZT}$ composites.

trical resistance. The piezoelectric constant of the composites decreases with the decrease in the volume fraction of PZT.

Fig. 8 shows magnetostriction measured for the NFO/PZT composites. The longitudinal magnetostriction λ_{11} is measured

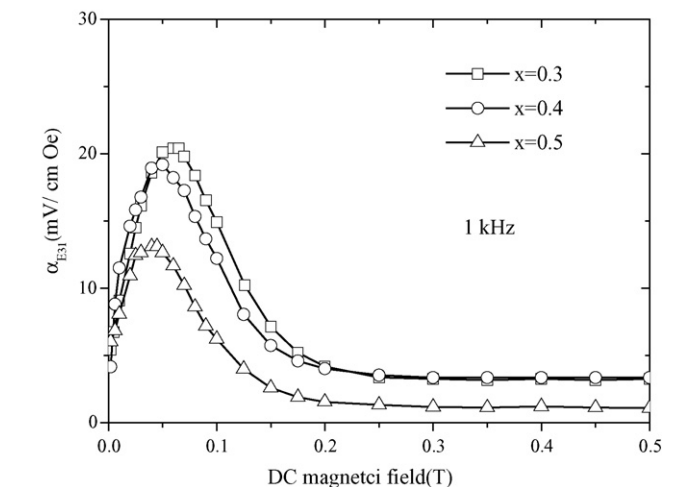
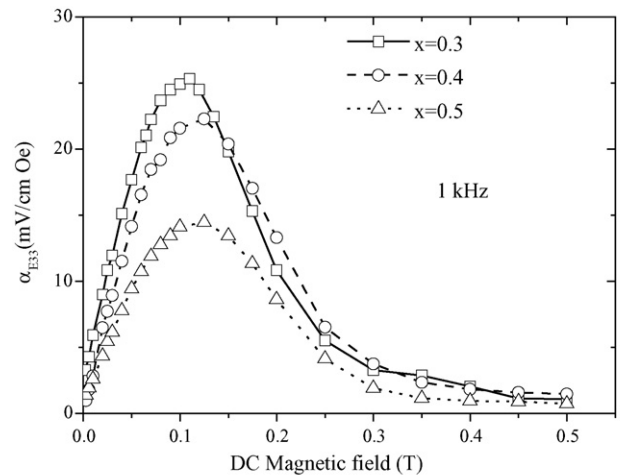


Fig. 9. Bias magnetic field H dependence of magneto-electric voltage coefficients (α_{E33} , α_{E31}) for $x\text{NFO}/(1-x)\text{PZT}$ composites.

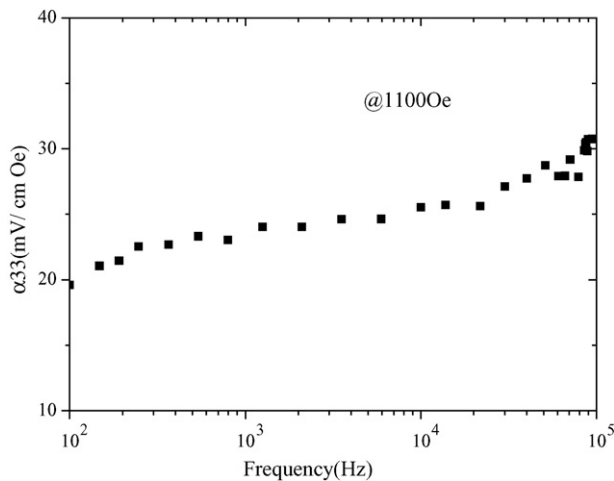


Fig. 10. A typical frequency dependence of α_{E33} for 0.3NFO/0.7PZT composites.

when the strain foil is parallel to the magnetic field, and the transverse magnetostriction λ_{13} is obtained when the strain foil is perpendicular to the magnetic field. The absolute values of λ first increase rapidly with the applied magnetic field and then approaches its saturation at high magnetic field. The saturation magnetostriction increases with the content of NFO.

The magnetic field dependence of ME coefficients α_E with different PZT content is shown in Fig. 9. At the same dc magnetic field, the values of α_E reduce with the PZT content because of the difficult polarization and higher porosity of the ceramics as show in Table 1. For the same sample, α_{E31} is a bit larger than α_{E33} . This characteristic is related to the field dependent magnetostriction shown in Fig. 8. $q_{11} = d\lambda_{11}/dH$ reaches its saturation at 1.1 kOe, and q_{13} reaches its saturation at 0.9 kOe.

A typical frequency dependence of ME coefficient is shown in Fig. 10. The ME effect increases slowly with the frequency below 100 kHz. ME constant has an inverse ratio to dielectric constant and capacitance according to formula (1).

4. Conclusions

Dense composites consisting of ferromagnetic and ferroelectric phases have been prepared by SPS consolidation of mechanically mixed powder mixtures. The assemblage of PZT and NFO

is a feasible combination as inter-phase diffusion and possible chemical reaction are readily retarded in this composite system. The SPS condition has an essential influence on the magnetic dielectric properties.

Acknowledgements

This work was supported by the grants sponsored by the National Science Foundation of China through grant 50318002, 50328203 & 10574078, the Ministry of Sciences and Technology of China through grant No. 2002CB613303, and the Swedish Research Council through grant 621-2002-4299.

References

1. Fiebig, M., Revival of the magnetoelectric effect. *J. Phys. D: Appl. Phys.*, 2005, **38**, R123–R152.
2. Wang, J., Neaton, J. B., Zheng, H., Nagarajan, V., Ogale, S. B., Liu, B. et al., Epitaxial BiFeO₃ multiferroic thin film heterostructures. *Science*, 2003, **299**(5613), 1719–1722.
3. Goto, T., Kimura, T., Lawes, G., Ramirez, A. P. and Tokura, Y., Ferroelectricity and giant magnetocapacitance in perovskite rare-earth manganites. *Phys. Rev. Lett.*, 2004, **92**(25), 257201.
4. Hur, N., Park, S., Sharma, P. A., Guha, S. and Cheong, S. W., Colossal magnetodielectric effects in DyMn₂O₅. *Phys. Rev. Lett.*, 2004, **93**(10), 107207.
5. Van Suchtelen, J., Product properties: a new application of composite materials. *Philips Res. Rep.*, 1972, **27**, 28–37.
6. Lottermoser, T., Lonkai, T., Amann, U., Hohlwein, D., Ihringer, J. and Fiebig, M., Magnetic phase control by an electric field. *Nature*, 2004, **430**(6999), 541–544.
7. Nan, C. W., Magnetoelectric effect in composites of piezoelectric and piezomagnetic phases. *Phys. Rev. B*, 1994, **50**(9), 6082–6088.
8. Zhai, J. Y., Cai, N., Shi, Z., Lin, Y. H. and Nan, C. W., Coupled magnetodielectric properties of laminated PbZr_{0.53}Ti_{0.47}O₃/NiFe₂O₄ ceramics. *J. Appl. Phys.*, 2004, **95**(10), 5685–5690.
9. Harshe, G., Dougherty, J. P. and Newnham, R. E., Theoretical modeling of 3-0/0-3 magnetoelectric composites. *Int. J. Appl. Electromagn. Mater.*, 1993, **4**(2), 161–171.
10. Ryu, J., Carazo, A. V., Uchino, K. and Kim, H. E., Piezoelectric and magnetoelectric properties of lead zirconate titanate/Ni-ferrite particulate composites. *J. Electroceram.*, 2001, **7**(1), 17–24.
11. Shen, Z. and Nygren, M., Microstructural prototyping of ceramics by kinetic engineering: Applications of spark plasma sintering. *Chem. Record*, 2005, **5**(3), 173–184.
12. Zhai, J. Y., Cai, N., Shi, Z., Lin, Y. H. and Nan, C. W., Magnetic-dielectric properties of NiFe₂O₄/PZT particulate composites. *J. Phys. D: Appl. Phys.*, 2004, **37**(6), 823–827.